

Performance limitations of niobium-based submillimeter-wave quasiparticle mixers operating near the gap frequency.

P. Hebre*, M. Salez, W. R. McGrath, B. Bumble, and H. G. LeDuc

Center for Space Microelectronics Technology, Jet Propulsion Laboratory,
California Institute of Technology, 4800 Oak Grove Dr., Pasadena, CA 91109

*DEMIRM - Observatoire de Paris-Meudon, 5 place Jules Janssen, 92195 Meudon, France

We have measured the noise temperature of heterodyne receivers employing Nb/AIO_x/Nb tunnel junction mixers at frequencies ranging from 70% to 93% of the gap frequency of niobium (~700 GHz). The sensitivity of the receiver is decreased by the overlap of the $n = 1$ and $n = 2$ photon steps of opposite sign. At bias voltages where these photon steps overlap, there is an increase in receiver noise of up to 50%. Theoretical calculations using the Tucker theory agree well with the observed mixer performance. This overlap already affects the receiver operation for best performance at frequencies well below 700 GHz.

Low-noise heterodyne receivers using quasiparticle SIS (Superconductor-Insulator-Superconductor) tunnel junction mixers operating at millimeter and submillimeter wavelengths have been developed primarily for radioastronomy applications.¹⁻⁷ The SIS mixers, for which the Tucker mixer theory⁸ predicts high RF-to-IF conversion efficiency and quantum-limited noise, are expected to work well at frequencies up to the gap frequency of the superconductor used, and up to twice that frequency with somewhat degraded performance.⁹⁻¹⁰ Almost all SIS receivers presently used on radiotelescopes employ niobium tunnel junctions for their ruggedness and high quality I - V characteristics. Recently, a few receivers using niobium mixers have been developed^{2-5,7} for frequencies approaching 700 GHz, the gap frequency of niobium. Mixer operation above the gap frequency of Nb has been demonstrated in the laboratory⁶, but with significantly worse performance. While some preliminary measurements have also been done on low energy gap superconductors, like aluminum,¹¹ at millimeter wavelengths, little has been done to investigate at submillimeter wavelengths the consequences of operating SIS receivers near the energy gap.

One consequence, expected theoretically for operation near the gap frequency, is an increase of the receiver noise at bias voltages where the $n = 1$ photon step of the positive voltage region in the I - V curve and $n = 2$ photon step from the negative voltage region overlap. As shown in Fig. 1, the $n = 2$ photon step decreases the i - I -induced (pumped) current in the overlap range, causing a change of slope in the pumped I - V curve. Subsequently, a minimum is expected in the receiver IF output power at this change of slope, as a result of the smaller IF dynamic impedance which increases the IF mismatch and the mixer conversion loss.¹² The frequency at which an overlap starts shrinking the bias region on the first photon step is:

$$f = \frac{2}{n+1} f_g \quad (1)$$

where n is the order of the photon step of opposite sign and f_g is the gap frequency. One sees that the $n = 3$ photon step starts playing a role at $f > 350$ GHz ($f > f_g/2$ where $f_g = 700$ GHz for Nb), but for practical local oscillator (L.O) powers, the effect is negligible. The case $n = 2$ occurs for $2/3 f_g < f < f_g$, i.e. for frequencies between 466 GHz and 700 GHz. We have investigated experimentally and theoretically how this $n = 2$ case overlap affects the sensitivity of a submillimeter-wave receiver. This effect has not been mentioned in the literature so far, possibly because few SIS receiver results have been reported in

this frequency range.

Two heterodyne receivers designed for astronomical observations at 547 GHz and 626 GHz, have been used to study SIS mixer performance at frequencies between 490 GHz and 650 GHz, i.e. 70% to 93% of the gap frequency of niobium. Both receivers use similar waveguide mixers, and an extensive discussion of their design has been provided elsewhere.^{5,7} The SIS mixers each use a single $0.25 \mu\text{m}^2$ area Nb/Al-AIO_x/Nb tunnel junction.¹³ To optimize the RF impedance match, the waveguide backshort and E-plane tuner are used in conjunction with a superconductive micro strip circuit integrated with the junction to provide an appropriate embedding circuit. The double-sideband (DSB) receiver noise temperature is derived from $T_R = (T_h - Y T_c) / (Y I)$ where Y is the ratio of the IF output powers measured in response to a hot ($T_h = 290$ K) and a cold ($T_c = 82$ K) load placed at the receiver RF input.

Figure 2 shows the receiver IF output power for the RF hot and cold load signals as a function of bias voltage for 4 different L.O frequencies: 490, 540, 631 and 649 GHz. One notices a sharp minimum in the IF power occurring at a voltage which increases with frequency. In addition, the L.O-pumped I - V curves which are also shown in Fig. 2 display a change of slope for the same voltage. We contend that the change of slope in the pumped I - V curves and the sharp minimum in the IF power curves both result from the overlap of the $n = 1$ and $n = 2$ photon steps discussed above. The fact that high L.O powers enhance the effect supports this interpretation. The

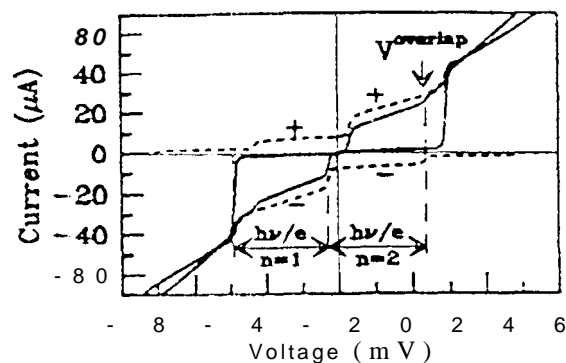


Fig. 1. Schematic reconstruction of an experimental pumped I - V curve displaying an inflection point (solid line) using the photon step overlap argument. The dashed curves show the photon steps of width $h\nu/e$ from the positive and negative voltage regions "before" their effects are added.

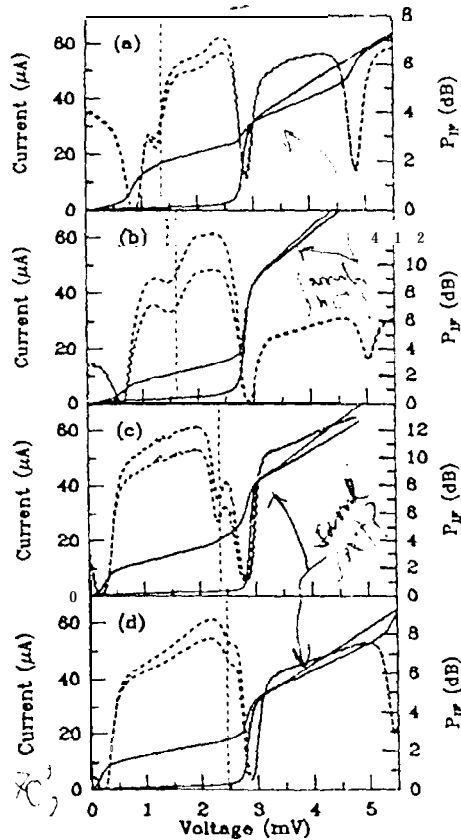


Fig. 2. Unpumped and I.O. pumped I - V curves and IF output power for hot and cold load signals versus bias voltage for a few different junctions at (a) $f = 490$ GHz; (b) 540 GHz; (c) 631 GHz; and (d) 649 GHz. The dashed vertical lines indicate V_{overlap} .

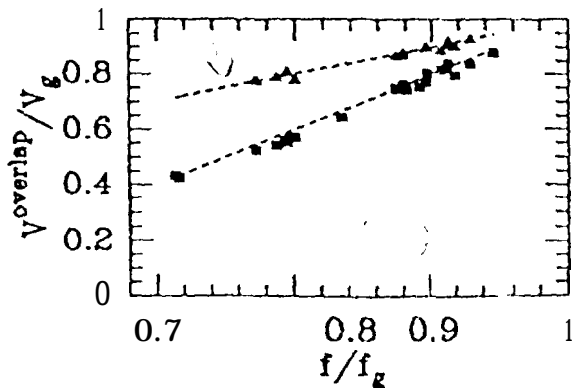


Fig. 3. Measured voltages for the inflection point (squares), normalized to the gap voltage $hf_g/2e$, as a function of the normalized I.O. frequency f/f_g . The dashed line represents the predicted voltages for the photon step overlap. For comparison, the 2nd Shapiro steps (triangles) are also shown and compared to the Josephson voltage-frequency relation $v_{\text{shapiro}} = 2(hf/2e)$ (dotted line).

measured voltages for which the change of slope occurs in the pumped I - V characteristics are plotted versus I.O. frequency in Fig. 3. It can be seen that they are highly correlated with the overlap voltages given by:

$$V_{\text{overlap}} \approx 2 hf_g/e \cdot V_g \quad (2)$$

Moreover, this feature is magnetic-field insensitive, which rules out Josephson-type phenomena. The $n=2$ Shapiro step is seen as an independent component and can be quenched by a magnetic field applied in the plane of the junction. It has been measured versus I.O. frequency and as seen in Fig. 3 is clearly distinct from the photon step overlap.

The receiver performance was optimized with respect to backshort, E-plane tuner, and I.O. power on the peak in the IF output at a bias voltage above V_{overlap} . The receiver noise temperature was then measured at this point and a bias below the overlap voltage without re-optimizing the mixer. For the 600 GHz receiver, the best performance between 610-631 GHz is 214-240 K. The noise temperature is higher by 40-64 K respectively (i. e., 17-30%), at the best bias point below V_{overlap} . The variations exhibited by the observed noise temperatures and their increases are caused by the exact settings of the waveguide tuners and I.O. power rather than by a systematic trend with frequency. The second receiver operated at 540 GHz gives a noise temperature of 196 K and shows an increase of 108 K (55%) below the overlap voltage. Such a receiver noise increase implies integration times longer by a factor of up to 2.5 for actual astronomical observations.

We have performed calculations using the Tucker theory⁸ to analyze the observed change of slope in the pumped I - V curves, and to investigate the predicted effect on the mixer noise temperature T_M and conversion efficiency G_M . The theory is fitted to the pumped I - V curves using the I.O. voltage amplitude as a free parameter to obtain the embedding impedance of the mixer circuit. Calculated pumped I - V curves can then be generated for any I.O. pump level, along with the corresponding values of G_M and T_M . The measured noise and gain of the IF system have also been included to predict the total receiver noise and the IF output power for the hot RF load signal.

Figure 4 (a) shows a calculated pumped I - V curve fitting experimental data at 540 GHz⁷ (the fitted and experimental curves are barely distinguishable). The fitted embedding impedance is $Z = 58 - j105 \Omega$ and the I.O. power is 50 nW, close to [the optimum for best receiver performance. The calculated IF output power for the RF hot load signal] is also shown in Fig. 4 (a) and agrees reasonably well with the measured IF output power. The IF system noise was 7 K for this receiver and the noise contribution of the elements located in front of the mixer have not been considered in the calculation, which partly explains the difference in measured and calculated receiver noise temperatures shown in figure 4 (b). While the theory underestimates the actual noise, it nevertheless predicts a significant increase in noise below the overlap. The calculated available and coupled mixer gain are plotted in Fig. 4 (c) and show that the dip observed in the IF output power at V_{overlap} corresponds to a sharp decrease of the available mixer gain, and is only weakly dependent on the IF mismatch. A similar set of curves is shown in Figs. 4 (d), (e) and (f) for an I.O. frequency of 631 GHz.⁸ The embedding impedance to achieve a good fit to the I - V curve is $Z = 28.3 - j52.3 \Omega$, the estimated I.O. power is 100 nW, and the IF noise temperature is 4 K. Qualitatively and quantitatively, the overall agreement between the calculated and measured receiver noise variations is quite good.

As frequency is increased, the voltage range $V_{\text{overlap}} < V < V_{\text{gap}}$ for best performance (above the dashed line in Fig. 3) is reduced to a small region corresponding to a very narrow peak in the IF power curve (see Fig. 2(c)), which vanishes completely near 700 GHz. At frequencies above 650 GHz, this region is exceedingly small, allowing no practical bias at $V > V_{\text{overlap}}$, and the effect discussed here would be unnoticed.² In this case the mixer would be optimized in the overlap region. We have calculated the optimized receiver performance at biases both above and below V_{overlap} . The theory suggests that optimized receiver noise below V_{overlap}

would be about 22% higher than above at 630 GHz; and the change would be 35% at 540 GHz.

Furthermore as frequency increases, the second Shapiro step and the overlap voltage converge putting the optimum bias near the Shapiro step. This is not a problem around 547 GHz where a large part of the photon step can still be used, but becomes of concern near 600 GHz and above. Therefore, strong suppression of the AC Josephson effect with an external magnetic field is critical to avoid instabilities and additional noise. While it is possible in theory to quench the Shapiro steps by applying a suitable magnetic field, noise spikes often remain in the actual IF power curves no matter how smoothed the $I-V$ characteristics appear (see Fig. 2(c)). While applying additional flux quanta, $\Phi_0 = h/2e$, may improve the IF response, the intense magnetic field has the undesirable effect of slightly decreasing the gap voltage. This increases V_{overlap} according to eqn. (2), further decreasing the desirable bias range. For an applied field resulting in $\Phi \approx 3\Phi_0$ in our junctions, we find $V_{\text{reduced}} - V_{\text{overlap}}$ already at only 635 GHz, indicating that the bias region where there is no overlap has disappeared.

Above 700 GHz, the performance of niobium-based SIS mixers is reasonably good¹⁴ although slightly degraded because the $n=1$ and $n=2$ photon steps now completely overlap. In addition, the mixer can only be operated at $V > h\omega/e - V_g$ because of the overlapping $n=1$ photon step from the negative region. The upper limit for niobium SIS mixers is about 1400 GHz, twice the gap frequency, when the $n=1$ photon step from either side covers the entire $(-V_g, V_g)$ bias range.

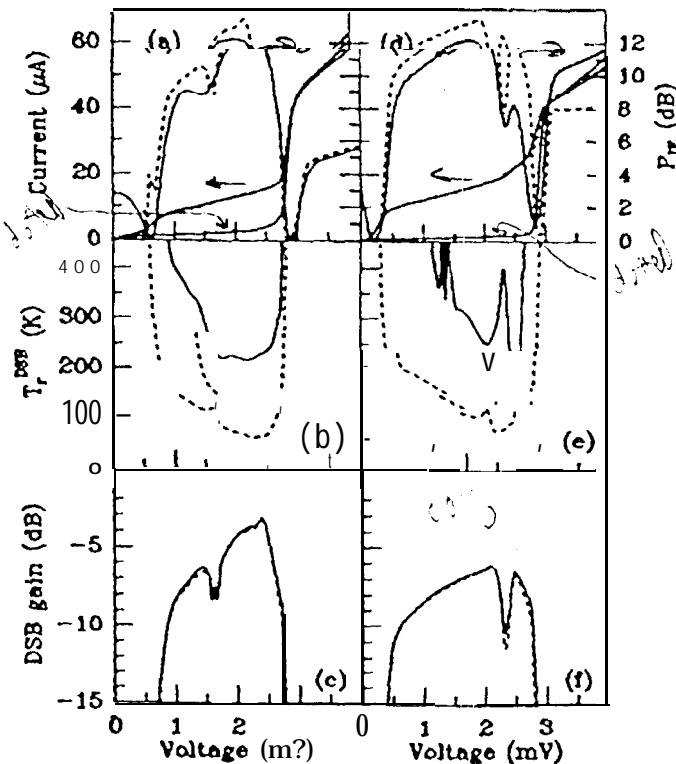


Fig 4. (a) Measured (solid) and calculated (dashed) pumped $I-V$ curves, measured (solid) and calculated (dashed) IF power for hot load signal at 540 GHz; (b) measured (solid) and theoretical (dashed) double-sideband T_{rec} versus bias voltage at 540 GHz; (c) calculated available (solid) and coupled (dashed) mixer gains at 540 GHz; (d), (e) and (f): same set of curves at 631 GHz.

In summary, we have observed the effect of overlapping photon steps on SIS mixer performance at submillimeter wavelengths. The increase in receiver noise caused by this effect can already become difficult to avoid at frequencies as low as 635-650 GHz, which is still well below the gap frequency of Nb.

The research described in this paper was performed by the Center for Space Microelectronics Technology, Jet Propulsion Laboratory, California Institute of Technology, and was jointly sponsored by the Innovative Science and Technology Office of the Ballistic Missile Defense Organization and the National Aeronautics and Space Administration, Office of Space Access and Technology and the Office of Space Science. M. Salez is currently sponsored by the Research Associateship Program of the National Research Council.

- 1 A. Karpov, J. Blondel, B. Lazareff, K. H. Gundlach, Proc. 5th Int. Symp. on Space Terahertz Technology, p. 73, Univ. of CA, Los Angeles (1993).
- 2 J. Kooi, C.K. Walker, H. G. LeDuc, T.R. Hunter, D.J. Benford, J.G. Phillips, Int. J. of Infrared and Millimeter Waves 8, 1287 (1994).
- 3 J. Zmuidzinas, H.G. LeDuc, J.A. Stern, S.R. Cypher, IEEE Trans Microwave Theory Tech 42, 098 (1994).
- 4 J. Mees, S. Crewell, H. Nelt, G. de Lange, H. van de Stadt, J.J. Kuipers, R.A. Panhuizen, Proc. 5th Int. Symp. on Space Terahertz Technology, p. 142, Univ. of MI, Ann Arbor (1994).
- 5 M. Salez, P. Febyre, W.R. McGrath, B. Bumble, H. G. LeDuc, Int. J. of Infrared and Millimeter Waves 15(6), 349 (1994).
- 6 G. de Lange, C.E. Honingh, M. M.T. M. Dierichs, H.H. A. Schaeffer, H. Kuipers, R. A. Panhuizen, J. M. Klapwijk, H. van de Stadt, M.W.M. de Graauw, E. Armandillo, Proc. 4th Int. Symp. on Space Terahertz Technology, p. 41, Univ. of CA, Los Angeles, (1993).
- 7 P. Febyre, W.R. McGrath, P. Batelaan, B. Bumble, H. G. LeDuc, S. George, P. Feautrier, Int. J. of Infrared and Millimeter Waves 15, 943 (1994).
- 8 J.R. Tucker, IEEE J. Quantum Electron., QE-15, 1234, (1979).
- 9 M.J. Feldman, Int. J. of Infrared and Millimeter Waves 8, 1287 (1987).
- 10 W.C. Danchi, J.C. Sutton, J. Appl. Phys 60, 3967 (1986).
- 11 J. Winkler and J. Claeson, J. Appl. Phys 62, 4482 (1987).
- 12 W.R. McGrath, P.I. Richards, A. J. Smith, H. van Kempen, R. A. Batchelor, Appl. Phys Lett 39, 655 (1991).
- 13 H.G. LeDuc, B. Bumble, S. R. Cypher, A.J. Judas, J.A. Stern, Proc. 3rd Int. Symp. on Space Terahertz Technology, p. 408, Univ. of MI, Ann Arbor (1992).